AAS 16-399

DEVELOPMENT OF A SATELLITE GROUP TRACKING METHOD

Christopher R. Binz* **and Liam M. Healy***

When multiple objects are orbiting in close proximity to one another, as in the early stages of a breakup or a deployment, conventional tracking is difficult because of the observation association problem. However, the ability to characterize and track these objects quickly is important for spaceflight safety. This paper explores the concept of group tracking for space surveillance. Explicit observation association is not required, as the "cloud" of objects is tracked as a parameterized collective. A scheme for tracking the centroid and extent parameters of the collection separately is presented, along with preliminary results.

INTRODUCTION

When multiple objects are orbiting in close proximity to one another, as in the early stages of a breakup or a deployment, conventional tracking methods can have difficulties because of the observation and track association problems. Although there are methods to mitigate these issues, they often rely on very high quality observations, increased sensor tasking, and large-scale parallel processing capabilities. Operationally, it often takes days or weeks to publish two-line element sets for an unexpected breakup (time spent waiting for the objects to separate enough to allow for unambiguous tracking), or to positively identify specific cubesats from a mass deployment.[1] Ephemeris error attributable to misidentification is often high in these cases, as well.[2]

A subset of the multiple target tracking literature deals with the concept of group tracking, in which closely-spaced or coordinated targets are tracked simultaneously as a cluster, instead of individually.[3,4,5] The original publications cite missile defense as the primary motivation,[3] but these techniques have not yet been applied to the space object tracking domain. The increasing frequency of debris-generating events, as well as the prevalence of large, near-simultaneous deployments of small satellites, is exposing the limitations of the current tracking methods.[1]

This paper explores the problem of estimating the parameters of a cluster of satellites using ground-based observations. The approach taken is to decouple the cluster centroid tracking (essentially a point target tracking problem) and the extent parameter estimation,[8,9] using additional ideas initially introduced by Koch.[5] The result is an estimate of the centroid state and covariance, as well as the shape and extent of the cluster. The latter is accomplished via a particle filtering approach, while the former can be accomplished with any nonlinear estimator. The intent of this paper is to show that it is feasible to provide accurate estimates of a group of closely-spaced objects, including not only the absolute state, but also the geometry of the group itself. A schematic of this approach is shown in Figure 1.

There has been a significant amount of published research regarding the debris-generating events, but the majority focus on developing analytical models for the structure of the debris cloud shortly

*Code 8233, Naval Research Laboratory, Washington, DC 20375-5355.

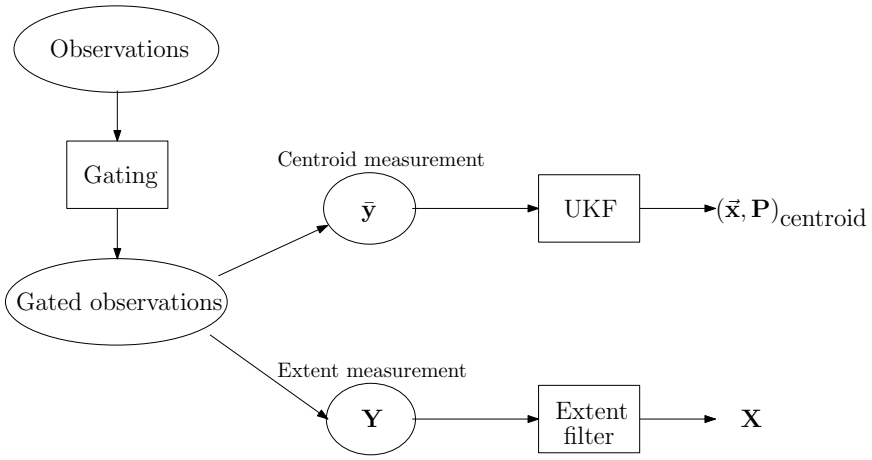

Figure 1: Overview of the group tracking method.

after the event.[10,11,12] This work approaches the problem from a tracking perspective, aiming to actively observe the structure of these debris clouds before the objects naturally separate—what Jehn calls phases C and D of a fragmentation event.[13]

The main motivation for tracking closely-spaced clusters of satellites as a group is that it obviates the need to wait for days or weeks for pieces to separate enough that they can be tracked individually. A space surveillance sensor network can be tasked more precisely on a quantified cluster, eliminating the need to search for pieces or correlate the observations to specific objects. In turn, spaceflight safety may be improved by the ability to provide a timelier assessment of a fragmentation event. Once the pieces naturally drift apart, the information about the cluster can be used to initialize the tracking of the constituent objects, potentially speeding the process of producing a high-accuracy orbit.

The paper is organized as follows: first, the parameterization of the cluster is explained. Then, the method for estimating these parameters is described. A simulated breakup is presented as a test case, and the extent parameter estimation performance is discussed. Forward work and alternative approaches to this problem are discussed at the end.

Cluster parameterization

The chosen parameterization for a cluster of satellites is a hyperellipsoid in state space. Prior work has shown that an uncertainty ellipsoid represented by the covariance matrix remains valid for the longest periods of time after epoch when the covariance is represented in equinoctial elements,[14,15] and so this work parameterizes the cluster in equinoctial element space: $(n, a_f, a_g, \chi, \psi, \lambda)$.[16] The orientation and dimensions of this six-dimensional hyperellipsoid is described by a symmetric, positive definite matrix $\boldsymbol{X}$ (the "extent matrix"), and the center is simply the estimated state of the centroid of the cluster $\hat{\boldsymbol{x}}$, such that [17, p. 692]

$$(\boldsymbol{x} - \hat{\boldsymbol{x}})^T \boldsymbol{X}^{-1} (\boldsymbol{x} - \hat{\boldsymbol{x}}) = 1. \tag{1}$$

Conceptually, the ellipsoid described by $\boldsymbol{X}$ is similar to the covariance of a given state estimate. However, there are several key differences. First, the covariance describes the uncertainty of the

state estimate, whereas the extent matrix describes a "surface" containing the members of the satellite cluster. Further, because we decouple the problem of estimating the centroid of the cluster from the problem of estimating its extent, both the covariance estimate and the extent matrix estimate may be used, with the expectation that the covariance will be significantly different from the extent. This enables precision tracking of the centroid with uncertainty similar to that of a single tracked object, while maintaining information about the spread of objects for sensor tasking and conjunction warnings.

As this work concerns estimating the unknown extent matrix $\boldsymbol{X}$ in a Bayesian framework, a prior distribution of $\boldsymbol{X}$ is required. The Inverse Wishart distribution is often used as the conjugate prior for an unknown covariance matrix, [18, p. 111] and in fact is used as the prior in other group tracking literature, with good results.[4,5]

The probability density function of an Inverse Wishart-distributed random matrix $\boldsymbol{Y} \sim \mathcal{IW}(\nu, \boldsymbol{\Psi})$ is [19, p. 272]

$$f(\boldsymbol{Y}) = \frac{|\boldsymbol{\Psi}|^{\frac{\nu}{2}}}{2^{\frac{\nu p}{2}} \Gamma_p\left(\frac{\nu}{2}\right)} |\boldsymbol{Y}|^{-\frac{\nu+p+1}{2}} \exp -\frac{1}{2} \text{ tr } (\boldsymbol{\Psi}\boldsymbol{Y}^{-1}), \tag{2}$$

where $\boldsymbol{Y}$ is a $p \times p$ positive definite matrix, $\boldsymbol{\Psi}$ is the scale matrix (also $p \times p$ and positive definite), and ν is the degree of freedom. The degree of freedom ν must be greater than $p + 1$, where p is the dimension of the matrix $\boldsymbol{\Psi}$. In this paper, it is chosen to be constant throughout the estimation process, with a value of $\nu = 9$.

One important property of this distribution that is leveraged here is the expected value [19, p. 273]:

$$\mathrm{E}[\boldsymbol{Y}] = \frac{\boldsymbol{\Psi}}{\nu - 6 - 1}. \tag{3}$$

MEASUREMENT PROCESSING

Gating

Observation gating refers to the process of choosing which observations to include for consideration in a data association problem. In this case, it refers to choosing the set of observations to be considered when computing the centroid and extent of the measurement set. Observations which are well-separated from the rest of the group should be processed as a separate target. Likewise, any clusters of observations which are clearly separate from the presently tracked group should be processed separately.

As an aside, the process of gating sets of discrete observations may or may not be applicable to a given situation. For instance, in the hypothetical tracking problem first posed by Segerman et al.,[1] any returns at all may be on a cluster of very small objects whose constituents are not observable on their own. In this case, the gating step is obviated by the fact that any objects that are separate from the cluster are not being observed in the first place.

This work uses the gating process first described by Drummond, et al.[3] First, an ellipsoidal gate S_G is constructed by combining—in measurement space—the predicted extent at time t_k, the expected measurement covariance of a single given observation R, and the covariance of the centroid state estimate P:

$$S_G = H\boldsymbol{X}_k^- H^T + R + HPH^T. \tag{4}$$

Typically, the size of the gate S_G is dominated by the extent contribution $H\boldsymbol{X}_k^- H^T$, although this could change with very tight clusters or very noisy sensors.

Once S_G is computed, the Mahalanobis distance[21] of each observation is calculated and compared to the chosen gate size g:

$$\sqrt{(\boldsymbol{y}_i - \boldsymbol{y}^-)^T S_G^{-1} (\boldsymbol{y}_i - \boldsymbol{y}^-)} \leq g, \tag{5}$$

where $\boldsymbol{y}^-$ is the predicted observation corresponding to the centroid of the group. Observations that do not satisfy Equation (5) are rejected, and not considered to be part of the group. The value chosen for g may be tuned based on the problem at hand; this paper uses $g = 1$ throughout.

Extent Observations

The gated set of measurements is now assumed to belong to the cluster of interest. This set may consist of any combination of returns from a single constituent object in the cluster, multiple returns from the same object, or false returns. For this initial study, the probability of a false return is assumed to be zero.

The centroid target state needs to be updated with the centroid of the measurement set, computed simply by taking the sample mean of the gated set, denoted $\bar{\boldsymbol{y}}$.[20] Updating the cluster extent requires an observation of the extent projected into measurement space, which takes the form of a 3×3 matrix.

One way to compute the measurement extent is to begin by calculating the sample covariance of the set of measurements, denoted $\boldsymbol{Y}$. As we are interested in the ellipsoid that encloses all measurements, we now scale $\boldsymbol{Y}$ by the largest Mahalanobis distance of the set, where Mahalanobis distance of the ith measurement is defined as:

$$k_i = \sqrt{(\boldsymbol{y}_i - \bar{\boldsymbol{y}})^T \boldsymbol{Y}^{-1} (\boldsymbol{y}_i - \bar{\boldsymbol{y}})}. \tag{6}$$

Thus the extent observation is taken to be $(\max k_i)^2 \boldsymbol{Y}$ (see Figure 2).

CENTROID FILTER

Centroid measurements $\bar{\boldsymbol{y}}_k$ may be processed by an unmodified extended or unscented Kalman filter to provide estimates of the centroid state and covariance $(\boldsymbol{x}, P)$, as the assumptions required for those tools remain valid here. This paper uses the unscented Kalman filter (UKF), the details of which may be found elsewhere.[22,23]

PARTICLE FILTER

While Koch is able to derive a closed-form solution to the joint (centroid and extent) filtering problem,[5] he does so by making several assumptions and approximations, several of which cannot be applied here. As such, this paper begins with the core assumption that the symmetric, positive-definite extent matrix is Inverse Wishart-distributed, then uses particle filtering methods to approximate the likelihood and posterior distributions. Specifically, the sampling importance resampling (SIR) particle filter is applied here.[24] The relevant steps are described below.

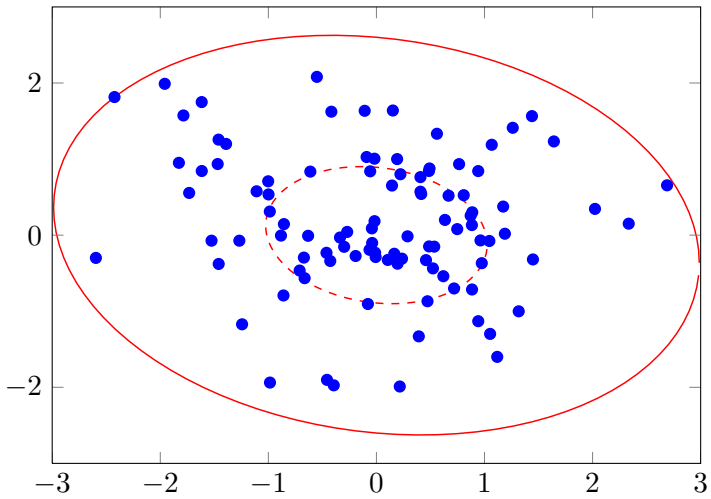

Figure 2: Example of covariance scaling. The 1σ covariance of this set of points is plotted with a red dashed line. The covariance scaled by the maximum Mahalanobis distance is plotted with a solid red line.

Prediction step

We begin with the assumption that the extent matrix at time step $k-1$ is Inverse Wishart-distributed:

$$\boldsymbol{X}_{k-1} \sim \mathcal{IW}(\nu, \boldsymbol{\Psi}), \tag{7}$$

where the scale matrix $\boldsymbol{\Psi}$ may be computed from the previous estimate of the expected value from the previous step $\boldsymbol{X}_{k-1}$: [19, p. 274]

$$\boldsymbol{\Psi} = (\nu - 6 - 1)\boldsymbol{X}_{k-1}. \tag{8}$$

In order to approximate the transition density and measurement likelihood, N samples (particles) are generated from this distribution. In the SIR framework, the distribution is resampled at every time step, so all particles begin with equal weights: $w_i = 1/N$. The work presented here uses $N = 10000$ particles.

Each particle $\boldsymbol{X}^i$ is propagated using the linearized state transition matrix $\boldsymbol{F}_k$ around the centroid solution $\boldsymbol{x}_{k-1}$:

$$\boldsymbol{X}_k^{i-} = \boldsymbol{F}_k \boldsymbol{X}_{k-1}^i \boldsymbol{F}_k^T. \tag{9}$$

Note that this is analogous to propagating the centroid covariance P, and could feasibly be done using, e.g., the unscented transform.

Update

Observations of the extent matrix are projections of the extent matrix into measurement space involving the nonlinear measurement function $h(\boldsymbol{X})$. This projection may be linearized around the current centroid state, yielding the matrix of partial derivatives for H for transforming between state space (equinoctial elements) and measurement space (range, azimuth, and elevation). Then,

each matrix-variate particle $\boldsymbol{X}^i$ may be transformed into measurement space using the similarity transformation:

$$\boldsymbol{Y}_k^i = \boldsymbol{H}\boldsymbol{X}_k^{i-}\boldsymbol{H}^T. \tag{10}$$

The particle weights w_i must be proportional to the measurement likelihood:

$$w_i \propto p(\boldsymbol{Y}^i|\boldsymbol{X}^i). \tag{11}$$

While the density of $\boldsymbol{X}_{k-1}$ is known *a priori*, the measurement likelihood is not, and so we must choose a function that is proportional to the measurement likelihood that we can evaluate. For this work, the inverse of the Frobeinus norm between the two matrices is used for this approximation. The Frobenius norm of a matrix A is defined as [25, p. 195]

$$||A||_F = \sqrt{\sum_{i=1}^{m}\sum_{j=1}^{n}|a_{ij}|^2}. \tag{12}$$

For this case, the metric is defined as the inverse of the Frobenius norm of the difference between the particle $\boldsymbol{Y}_k^i$ and the observed extent $\boldsymbol{Y}_k$:

$$\rho_i = 1/||\boldsymbol{Y}_k^i - \boldsymbol{Y}_k||_F. \tag{13}$$

As the results will show, this approach performs well. However, a focus of future work will be on refining this likelihood function.

The set of distances ρ are then used to construct the set of normalized weights:

$$w_i = \frac{\rho_i}{\sum_j^N \rho_j}. \tag{14}$$

A key consideration here is that while the distance metric is computed in measurement space, the weighted particles are combined in state space, in order to guarantee positive-definiteness. Rather than carrying the set of N particles through the next filtering step, $\boldsymbol{X}_k$ may be estimated by the weighted sum of particles. The updated extent matrix is then

$$\boldsymbol{X}_k = \sum_{i=1}^{N} w_i \boldsymbol{X}_k^{i-}. \tag{15}$$

Performance metric

In order to evaluate how well the extent matrix describes the actual extent of a cluster, we use the same Frobenius norm metric described earlier in Equation (12). More specifically, the Frobenius norm between the extent matrix $\boldsymbol{X}$ and some independent measure of the extent, with perfect knowledge of the simulated orbits of the constituent objects, is recorded.

A "true" extent against which to measure the estimated extent should have several properties. First, it should accurately reflect the definition of extent used in this paper: an ellipsoid representing the bounding surface that contains all of the objects in the cluster. Second, because of the nature of a closely-spaced cluster of satellites, it should be fairly insensitive to a small number of outliers,

which may be considered close to the cluster but are otherwise near the convex hull of the set of objects. These two properties are often at odds with each other, as the results will show.

One viable extent estimate is the sample covariance ellipsoid scaled to include all sample points. This involves the same calculation as the measurement extent (Equation (6)). It also has the two desirable properties identified earlier, with the exception of the scaling calculation. An object producing measurements near the very edge of the measurement gate will inflate this estimate, which will "snap back" once the object is separated enough to track individually.

The second separate measure of extent considered in this paper is the minimum volume enclosing ellipsoid (MVEE) over the full set of six-dimensional equinoctial states. Also known as the Löwner ellipsoid,[26] the idea is fairly self-explanatory: it is the smallest ellipsoid which bounds all points in the set. The algorithm published by Khachiyan[27] is used to compute the Löwner ellipsoid in this paper. His algorithm is not presented here, but it is described at length in the provided references.[26,27] This has the benefit of allowing the extent ellipsoid to simply "stretch" in one direction, rather than the symmetric scaling of the sample covariance. However, this method is very sensitive to outlier objects near the convex hull, as the simulation results will show. Figure 3 shows the Löwner ellipsoid plotted for an example set of points, along with the covariance ellipses.

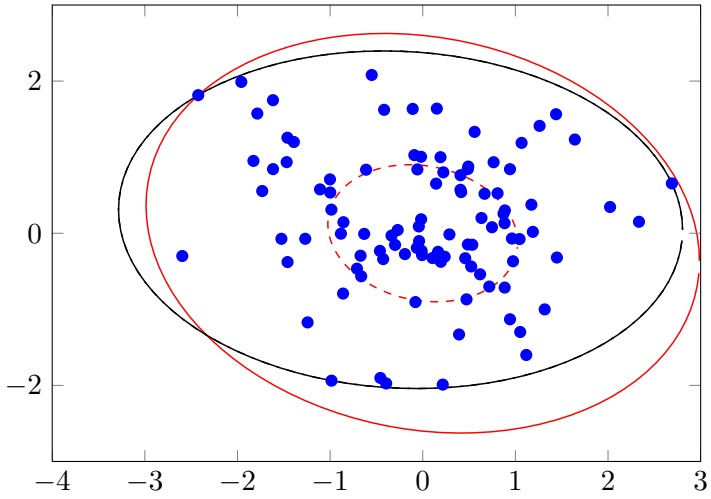

Figure 3: The Löwner ellipse is plotted with a solid black line, along with the unscaled and scaled covariance ellipses in Figure 3.

SIMULATION

A simulated breakup scenario is used here to demonstrate the group tracking technique described. The pre-breakup orbit parameters are listed in Table 1. The NASA standard breakup model is used to randomly generate fragments with a minimum characteristic length of 10 cm,[28] varying both the ΔV vector and the area to mass ratio of the fragments. The breakup epoch is set to be 1 January 2000 at 00:00:00 UTC. A ground station at sea level at 8°N, 5°E observes the debris cloud within five minutes after the breakup, when the pieces are still in close proximity with one another. 205 pieces are generated from the breakup simulation.

The ground station measures azimuth, elevation, and range to each fragment. For the purposes of this simulation, the sensor is assumed to have infinite resolution (i.e., measurements do not "merge"

Table 1: Pre-breakup orbit parameters used in the simulation.

a	6678.13 km
e	1.105×10^{-6}
i	28.5°
Ω	280.0°
ω	201.2°
ν	158.8°

with one another and are never missed). Zero-mean Gaussian noise is applied to the measurements, with $\sigma_{\text{azimuth}} = \sigma_{\text{elevation}} = 0.015°$ and $\sigma_{\text{range}} = 0.015$km.

The fragments are propagated via numerical integration, taking into account the effects of the J_2 zonal harmonic and atmospheric drag (using a simple exponential atmosphere model). Fragments with a perigee less than the radius of Earth are not considered. The resulting debris cloud is shown in Figure 4.

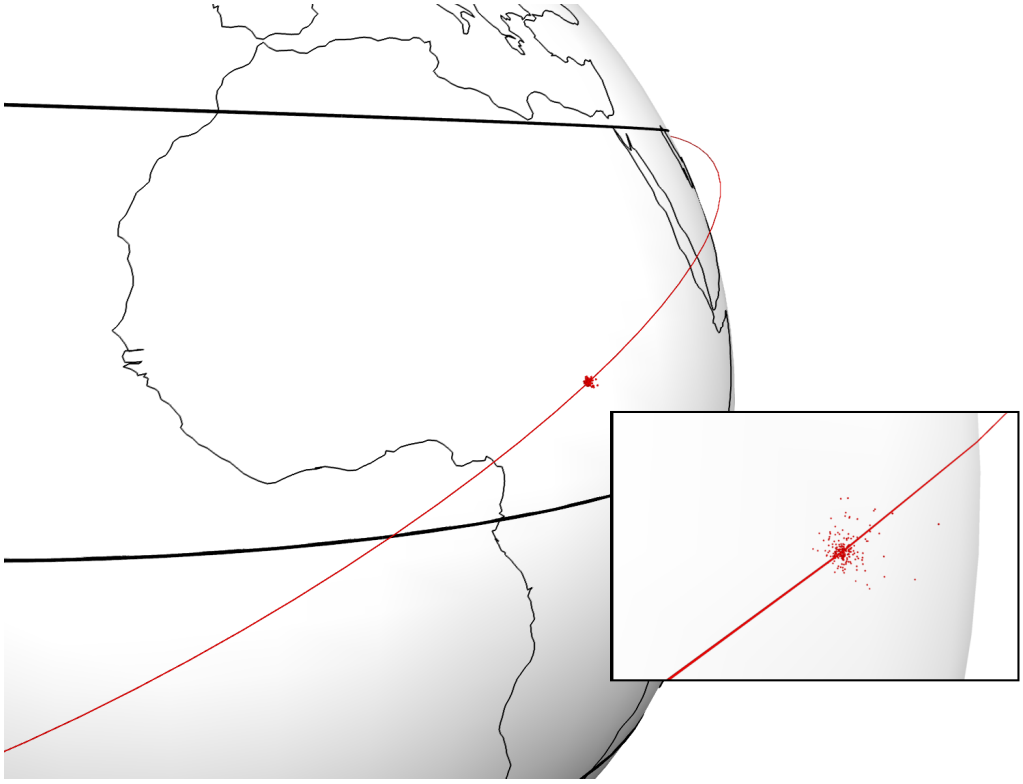

Figure 4: Debris cloud shortly after the fragmentation event, along with the original orbit track.

The state uncertainty of the reference (pre-fragmentation) orbit at the time of the fragmentation

event is conservatively assumed to be

$$P = \begin{bmatrix} 10 & 0 & 0 & 0 & 0 & 0 \\ 0 & 10 & 0 & 0 & 0 & 0 \\ 0 & 0 & 10 & 0 & 0 & 0 \\ 0 & 0 & 0 & 0.01 & 0 & 0 \\ 0 & 0 & 0 & 0 & 0.01 & 0 \\ 0 & 0 & 0 & 0 & 0 & 0.01 \end{bmatrix} \text{ km}^2/\text{s}^2, \tag{16}$$

where P is given in inertial Cartesian coordinates. This has no effect on the fragmentation event, but it allows us to initialize the extent matrix. In order to start with a very "wide" gate for accepting observations, we choose the initial value of the extent $\boldsymbol{X}_0 = 6P_{\text{eq}}$, where P_{eq} is the initial covariance matrix from above transformed into equinoctial element space.*

Results

The measurement residuals are plotted together with the 3σ covariance projected into measurement space in Figure 5. The behavior is mostly typical of a linearized Kalman filter such as the UKF. Further investigation into the dynamic behavior of the centroid can be found in a previous paper.[20]

Adding process noise to the prediction step improved both the centroid estimation and the extent estimation performance significantly. The process noise matrix used here is

$$Q = \begin{bmatrix} 1 \times 10^{-6} & 0 & 0 & 0 & 0 & 0 \\ 0 & 1 \times 10^{-4} & 0 & 0 & 0 & 0 \\ 0 & 0 & 1 \times 10^{-4} & 0 & 0 & 0 \\ 0 & 0 & 0 & 1 \times 10^{-4} & 0 & 0 \\ 0 & 0 & 0 & 0 & 1 \times 10^{-4} & 0 \\ 0 & 0 & 0 & 0 & 0 & 1 \end{bmatrix} \times 10^{-8}, \tag{17}$$

where Q is specified in equinoctial element space and units are consistent with n in $\frac{\text{rad}}{\text{sec}}$ and λ in radians. These values were chosen via trial and error.

Next, we examine the performance of the extent filter. Figure 6 shows the measurement gate S_G projected into the azimuth/elevation plane, along with the individual measurements at that time step. The extent estimate is initially very large with respect to the actual spread, leading the gating function to accept all associated observations. The gate forms a progressively tighter ellipse around the gated measurements as the filter processes more measurement frames. Note that rejected measurements that are inside the gating ellipse violate the range dimension of the gate, which is not shown here.

Figure 7 shows the evolution of the extent matrix itself, projected into mean motion/mean longitude space. Similar behavior can be seen here: more fragments are rejected from the group as the extent tightens around the core, closely-spaced cluster. Figure 8 shows projections of the entire 6D extent matrix at the end of the pass. Nearly all members of the cluster are contained within the extent ellipsoid, and it appears to represent the general shape of the cluster fairly well.

Figure 9 shows the Frobenius norm between the estimated extent matrix and the Löwner ellipsoid of the gated fragments, computed at each time step. There are occasional spikes in the value, which

*Covariance transformations are computed via the unscented transform.[29]

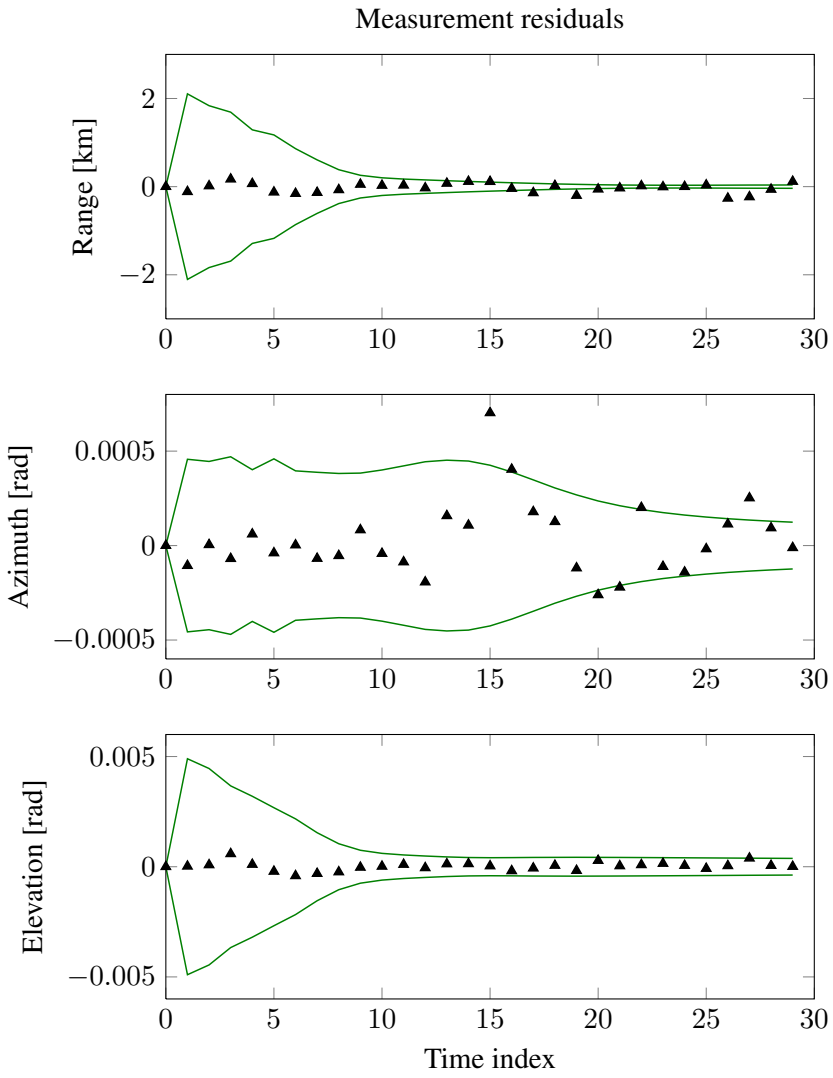

Figure 5: Centroid measurement residuals and 3σ bound.

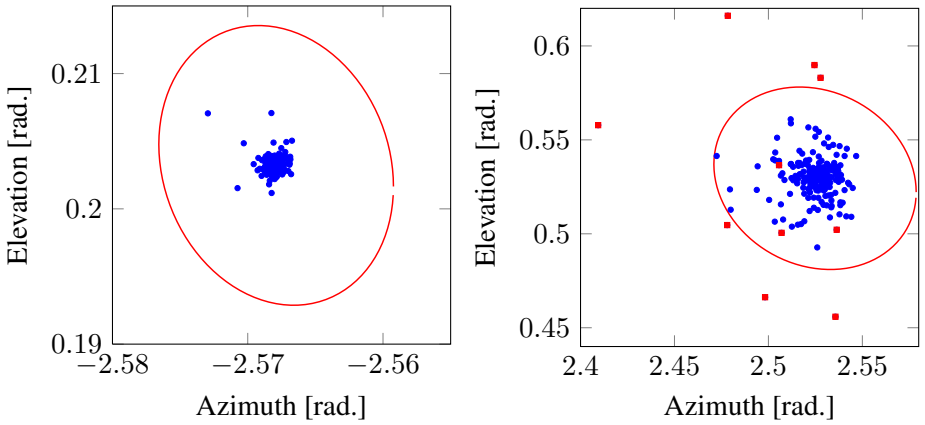

(a) Beginning of pass.

(b) Mid-pass.

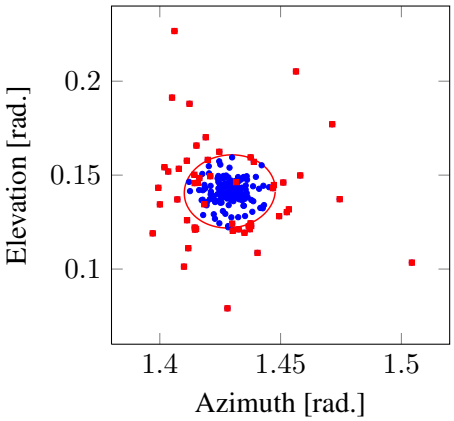

(c) End of pass.

Figure 6: Measurement gate evolution. Blue points are measurements accepted by the gating routine, red points are rejected measurements, and the red ellipse is the gate itself.

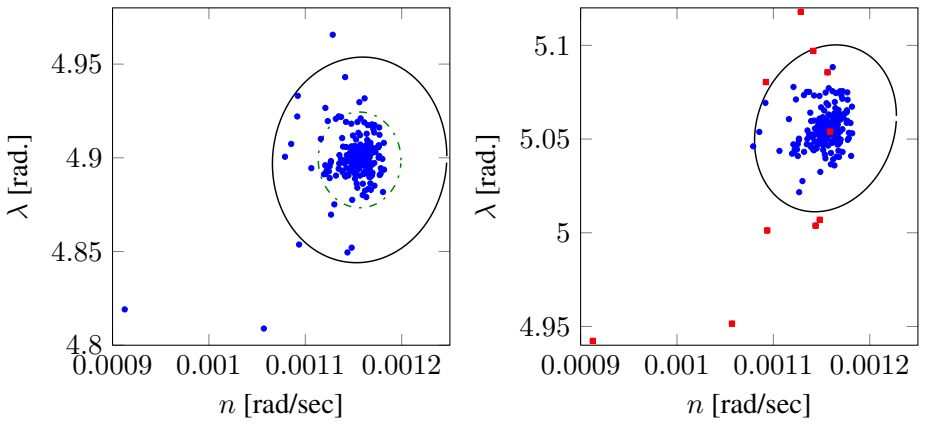

(a) Beginning of pass.

(b) Mid-pass.

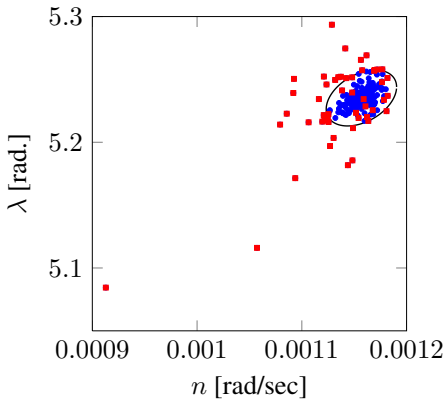

(c) End of pass.

Figure 7: Extent evolution projected in mean motion/mean longitude space. Blue points are accepted by the gating routine, and red points have been rejected. The black ellipse is the extent projection in n, λ space, and the dash-dotted line, visible only in the first plot, is the projected covariance of the centroid state.

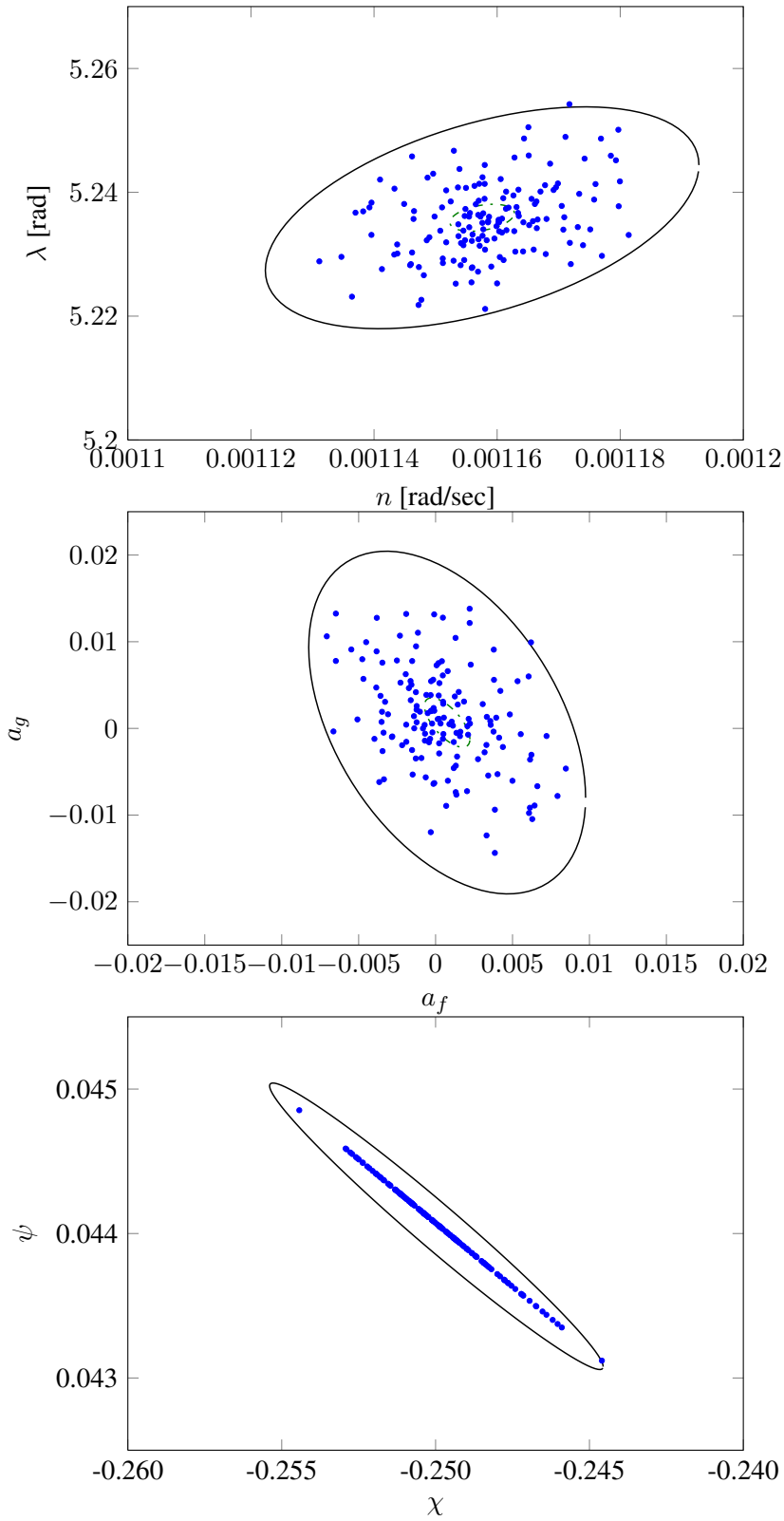

Figure 8: Extent matrix projections in state space, at the end of the pass. The extent is plotted with a solid black line, and each constituent satellite in the group is plotted with a blue dot. Objects producing rejected observations are not plotted.

could be related to the measurement gating step—one or more measurements being accepted when they are actually quite far from the cluster, or vice versa. The behavior of these values is likely caused by a problematic property of the Löwner ellipsoid: the fact that its size and shape are both very sensitive to single points—not necessarily outliers, but any point that is near enough to the convex hull of the set.

Figure 10 shows the Frobenius norm between the estimated extent matrix and the scaled sample covariance of the gated set of satellites at each time step. The initial extent matrix, which is set to be a multiple of the state covariance of the reference satellite, is a poor descriptor for the actual extent of the cloud of fragments, as evidenced by the relatively high Frobenius distance between it and the calculated measurement extent ellipsoid. Subsequent distances are significantly lower even after one or two processing steps, indicating that the extent filter is converging on a good description for the actual extent of the group.

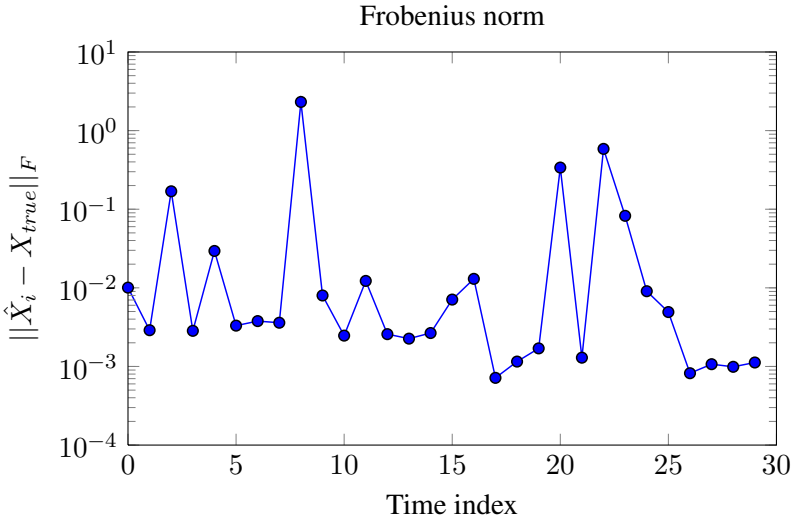

Figure 9: Fit metric using the Löwner ellipsoid, plotted with a log-scale y axis in order to preserve the detail of the plot.

One of the driving motivations for doing group tracking with satellites in the first place is to provide a mechanism through which ground assets may be tasked to observe the cluster of objects. As such, it's important to look at the performance of this technique over time spans longer than a single pass. Figure 11 shows the extent matrix projections after propagating for 3 hours after the breakup time.

The highly nonlinear nature of the high-drag reference orbit becomes more apparent here, particularly in mean motion/mean longitude space. Of course, extent propagation (without updates) over very long time periods is not critical, as the very nature of most fragmentation events means that these clusters are not long-lived, and the objects will tend to separate enough for individual tracking after days or weeks. However, over a typical propagation period, the extent matrix remains a valid descriptor of the actual cluster extent, as evidenced here.

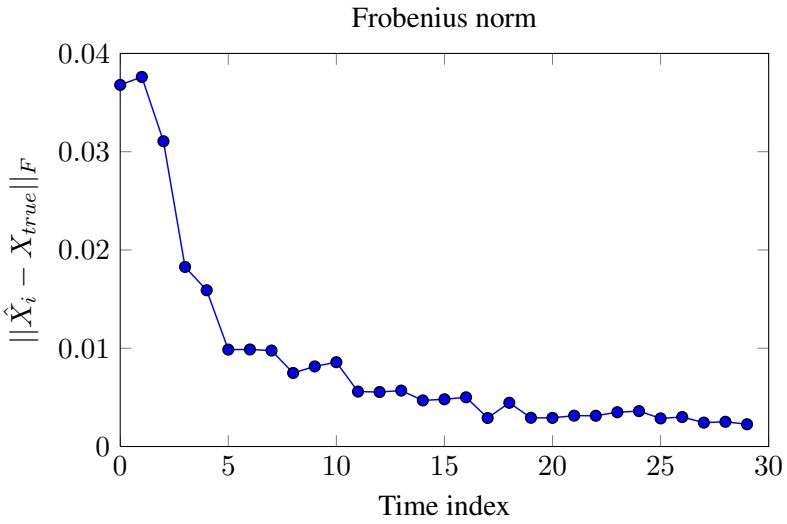

Figure 10: Covariance-based fit metric for the extent matrix.

SUMMARY AND CONCLUSIONS

This paper demonstrated the use of group tracking methods for ground-based space surveillance. The approach taken uses a synthesis of methods previously applied to the group tracking problem, including separating the centroid and extent estimation and modeling extent using random matrices. Measurements are gated according to the expected extent of the cluster, and no further measurement association is attempted, thus avoiding the difficulties plaguing current tracking methods, particularly against closely-spaced targets.

Once measurements are gated, a scaled sample covariance is used to describe observations of the cluster extent. Beginning with the assumption of an Inverse Wishart-distributed prior on the extent matrix in state space, a particle filter based on the Sampling Importance Resampling filter is used to update the extent matrix in a recursive estimation scheme.

Performance of this method was briefly explored via a simulated breakup scenario. The estimated extent is compared against the actual cluster extent (computed as the scaled sample covariance of the gated target set) using the Frobenius norm of the difference between the two matrices. As expected, this measure of error decreases with each subsequent filter step, similar to the uncertainty behavior in a typical nonlinear filtering problem.

FUTURE WORK

While this paper demonstrates the basic capability for tracking a cluster of satellites, there remains a significant amount of work to be done. A closed-form filter, similar to the one presented by Koch,[5] would be desirable as it would reduce computational requirements, but it remains to be seen if this type of solution exists. There are several potential improvements to be made to the particle filtering approach as well. The SIR particle filtering technique is likely sensitive to outliers,[24] so an alternative technique could improve performance.

Due to the novelty of this tracking approach, new ways of considering different space surveillance products, such as collision avoidance, sensor tasking, and initial orbit determination will need to be

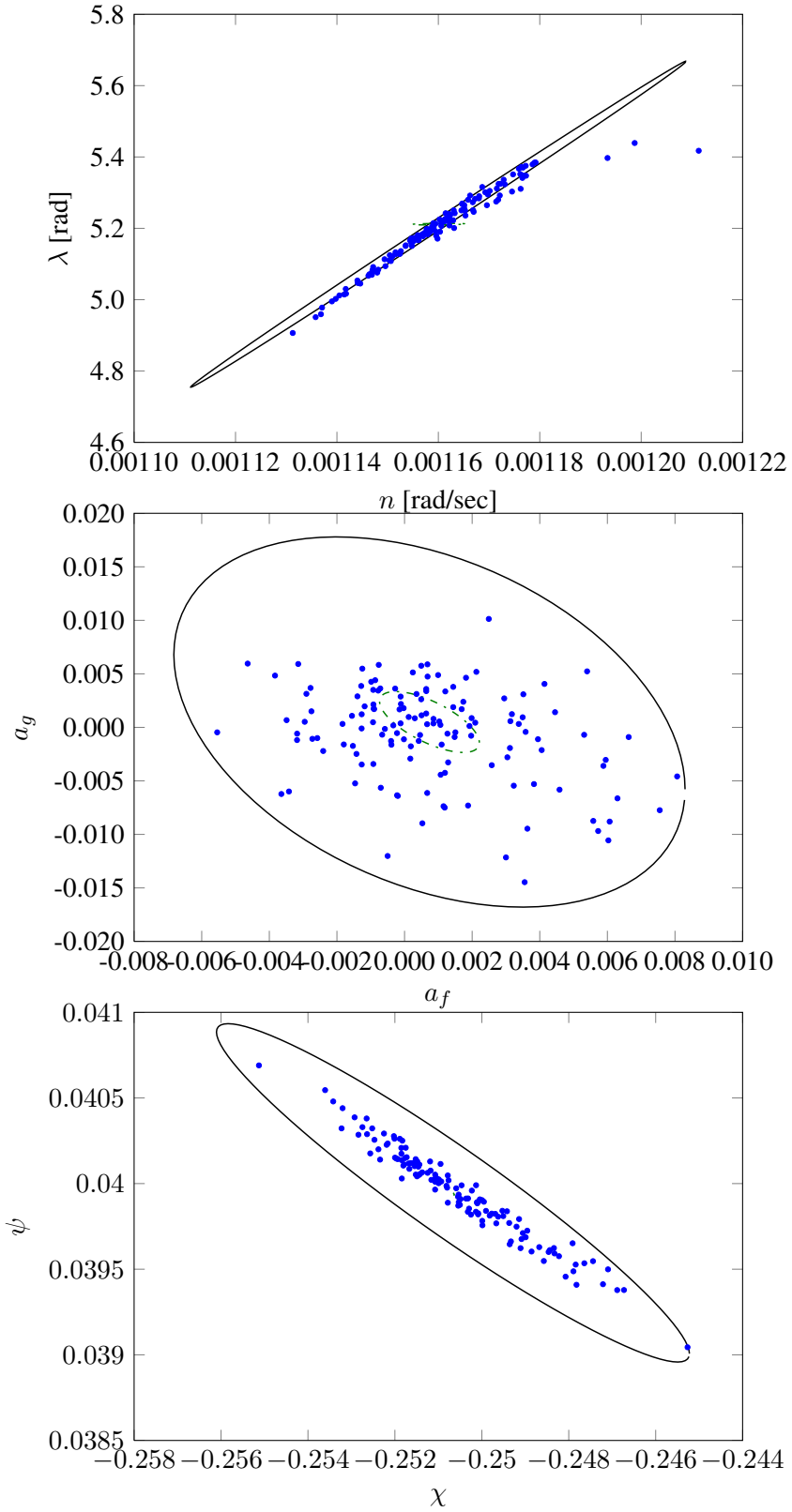

Figure 11: Extent matrix projections, propagated to 3 hours after the breakup time. Objects producing rejected observations are not plotted.

developed. Information about the cluster very soon after a deployment or fragmentation could be used to determine accurate orbits of individual pieces in a shorter amount of time than is currently feasible. Sensor tasking and acquisition for a cluster that may extend beyond the field of view of the sensor is a challenge that will need to be addressed as well.

REFERENCES

[1] A. Segerman, J. Byers, J. Emmert, and A. Nicholas, "Space Situational Awareness of Large Numbers of Payloads From a Single Deployment," *2014 AMOS Technical Conference, Wailea, Maui, HI*, 2014.

[2] K. Riesing, "Orbit determination from two line element sets of ISS-deployed cubesats," *Proceedings of the 29th Annual AIAA/USU Conference on Small Satellites*, 2015.

[3] O. E. Drummond, S. S. Blackman, and G. C. Pretrisor, "Tracking clusters and extended objects with multiple sensors," *Signal and Data Processing of Small Targets 1990*, Vol. 1305 of *Proceedings of SPIE*, 1990, pp. 362–375, 10.1117/12.21605.

[4] M. Feldmann, D. Franken, and W. Koch, "Tracking of Extended Objects and Group Targets Using Random Matrices," *IEEE Transactions on Signal Processing*, Vol. 59, Apr. 2011, pp. 1409–1420, 10.1109/TSP.2010.2101064.

[5] J. Koch, "Bayesian approach to extended object and cluster tracking using random matrices," *Aerospace and Electronic Systems, IEEE Transactions on*, Vol. 44, July 2008, pp. 1042–1059, 10.1109/TAES.2008.4655362.

[6] L. Bazzani, M. Cristani, and V. Murino, "Decentralized particle filter for joint individual-group tracking," *2012 IEEE Conference on Computer Vision and Pattern Recognition (CVPR)*, June 2012, pp. 1886–1893, 10.1109/CVPR.2012.6247888.

[7] G. Duan, H. Ai, S. Cao, and S. Lao, "Group Tracking: Exploring Mutual Relations for Multiple Object Tracking," *Computer Vision – ECCV 2012* (A. Fitzgibbon, S. Lazebnik, P. Perona, Y. Sato, and C. Schmid, eds.), No. 7574 in Lecture Notes in Computer Science, pp. 129–143, Springer Berlin Heidelberg, 2012.

[8] M. A. Zimmer and M.-J. Tsai, "Tracking of a single cluster of closely spaced objects using one and two passive optical sensors," *Signal and Data Processing of Small Targets 1992*, Vol. 1698 of *Proceedings of SPIE*, 1992, p. 268–280, 10.1117/12.139378.

[9] S. Blackman and R. Popoli, *Design and Analysis of Modern Tracking Systems*. Norwood, MA: Artech House, Inc., 1st ed., 1999.

[10] S. Barrows, G. Swinerd, and R. Crowther, "Review of debris-cloud modeling techniques," *Journal of Spacecraft and Rockets*, Vol. 33, No. 4, 1996, 10.2514/3.26798.

[11] R. Crowther, "Modeling the short-term evolution of orbital debris clouds in circular orbits," *Journal of Spacecraft and Rockets*, Vol. 31, No. 4, 1994, pp. 709–711, 10.2514/3.26502.

[12] R. K. Hujsak, "Nonlinear dynamical model of relative motion for the orbiting debris problem," *Journal of Guidance, Control, and Dynamics*, Vol. 14, No. 2, 1991, p. 460–465, 10.2514/3.20660.

[13] R. Jehn, "Dispersion of debris clouds from on-orbit fragmentation events," *ESA Journal*, Vol. 15, No. 1, 1991, pp. 63—77.

[14] C. Sabol, T. Sukut, K. Hill, K. T. Alfriend, B. Wright, Y. Li, and P. Schumacher, "Linearized orbit covariance generation and propagation analysis via simple Monte Carlo simulations," *Spaceflight Mechanics 2010*, Vol. 136 of *Advances in the Astronautical Sciences*, San Diego, CA, Univelt, Inc., 2010, pp. 509—526. AAS 10-134.

[15] J. T. Horwood, J. M. Aristoff, N. Singh, and A. B. Poore, "A comparative study of new non-linear uncertainty propagation methods for space surveillance," *Signal and Data Processing of Small Targets 2014*, Vol. 9092 of *Proceedings of SPIE*, 2014, pp. 90920H–90920H–24, 10.1117/12.2051353.

[16] J. R. Wright, "LS GEO IOD," *The Journal of the Astronautical Sciences*, Vol. 59, June 2012, pp. 352–369, 10.1007/s40295-013-0022-5.

[17] J. L. Crassidis and J. L. Junkins, *Optimal Estimation of Dynamic Systems*. Chapman & Hall/CRC Applied Mathematics & Nonlinear Science, Boca Raton, FL: CRC Press, second ed., 2011.

[18] A. K. Gupta and D. K. Nagar, *Matrix variate distributions*. No. 104 in Chapman & Hall/CRC monographs and surveys in pure and applied mathematics, Boca Raton, FL: Chapman & Hall, 2000.

[19] T. W. Anderson, *An Introduction to Multivariate Statistical Analysis*. Wiley Series in Probability and Statistics, Hoboken, NJ: Wiley, 3rd ed., 2003.

[20] C. R. Binz and L. M. Healy, "Centroid dynamics for group object tracking," *Space Flight Mechanics 2015*, Advances in the Astronautical Sciences, San Diego, CA, Univelt, Inc., 2015. AAS 15-365.

[21] P. C. Mahalanobis, "On the generalized distance in statistics," *Proceedings of the National Institute of Sciences (Calcutta)*, Vol. 2, 1936, pp. 49—55.

[22] S. Julier and J. Uhlmann, "New extension of the Kalman filter to nonlinear systems," *Signal Processing, Sensor Fusion, and Target Recognition VI*, Vol. 3068 of *Proceedings of SPIE*, July 1997, pp. 182–193. doi:10.1117/12.280797, 10.1117/12.280797.

[23] S. Särkkä, *Recursive Bayesian Inference on Stochastic Differential Equations*. Doctoral dissertation, Helsinki University of Technology, Helsinki, Finland, 2006.

[24] M. Arulampalam, S. Maskell, N. Gordon, and T. Clapp, "A tutorial on particle filters for online nonlinear/non-Gaussian Bayesian tracking," *IEEE Transactions on Signal Processing*, Vol. 50, Feb. 2002, pp. 174–188, 10.1109/78.978374.

[25] D. Kincaid and E. W. Cheney, *Numerical analysis: mathematics of scientific computing*. Pacific Grove, CA: Brooks/Cole, 3rd ed., 2002.

[26] M. J. Todd and E. A. Yıldırım, "On Khachiyan's algorithm for the computation of minimum-volume enclosing ellipsoids," *Discrete Applied Mathematics*, Vol. 155, Aug. 2007, pp. 1731–1744, 10.1016/j.dam.2007.02.013.

[27] L. G. Khachiyan, "Rounding of Polytopes in the Real Number Model of Computation," *Mathematics of Operations Research*, Vol. 21, No. 2, 1996, pp. 307–320.

[28] N. L. Johnson, P. H. Krisko, J. C. Liou, and P. D. Anz-Meador, "NASA's new breakup model of evolve 4.0," *Advances in Space Research*, Vol. 28, No. 9, 2001, pp. 1377–1384, 10.1016/S0273-1177(01)00423-9.

[29] S. J. Julier and J. K. Uhlmann, "Unscented filtering and nonlinear estimation," *Proceedings of the IEEE*, Vol. 92, 2004, p. 401–422.